# Responses to herbicides of Arctic and temperate microalgae grown under different light intensities

Juan Du, Disney Izquierdo, Hai-Feng Xu, Johann Lavaud, Leanne Ohlund, Lekha Sleno, Philippe Juneau

# Responses to herbicides of Arctic and temperate microalgae grown under different light intensities

Juan Du[a], Disney Izquierdo[b], Hai-Feng Xu[c], Beatrix Beisner[d], Johann Lavaud[e,f], Leanne Ohlund[g], Lekha Sleno[g] and Philippe Juneau[b*]

[a] Department of Biological Sciences, Université du Québec à Montréal-GRIL-TOXEN, Succ Centre-Ville, Montréal, Canada

[b] Department of Biological Sciences, Université du Québec à Montréal-GRIL-EcotoQ-TOXEN, Succ Centre-Ville, Montréal, Canada

[c] School of Life Sciences, and Hubei Key Laboratory of Genetic Regulation and Integrative Biology, Central China Normal University, Wuhan 430079, Hubei, China

[d] Department of Biological Sciences, Groupe de recherche interuniversitaire en limnologie (GRIL), Université du Québec à Montréal

[e] TAKUVIK International Research Laboratory IRL3376, Université Laval (Canada) - CNRS (France), Pavillon Alexandre-Vachon, 1045 av. de la Médecine, local 2064, G1V 0A6 Québec, Canada

[f] LEMAR-Laboratory of Environmental Marine Sciences, UMR6539, CNRS/Univ Brest/Ifremer/IRD, Institut Universitaire Européen de la Mer, Technopôle Brest-Iroise, rue Dumont d'Urville, 29280 Plouzané, France

[g] Chemistry Department, Université du Québec à Montréal-EcotoQ-TOXEN, Succ Centre-Ville, Montreal, Quebec, H3C 3P8, Canada

***Corresponding author:**

E-mail addresses: juneau.philippe@uqam.ca (P. Juneau)

Full postal address:

Department of Biological Sciences

Université du Québec à Montréal

CP8888, Succ Centre-Ville

Montréal (QC)

H3C 3P8

Canada

**Highlights**

- Photoadaptation processes are different between Arctic and temperate microalgae
- Arctic and temperate microalgae have different sensitivities to two herbicides
- High light enhances the impacts of herbicides on energy dissipation and photosynthesis of microalgae
- Atrazine removal by algae increased under high light
- These findings have applications for Arctic and temperate microalgae living in fluctuating light environments


## Abstract:

In aquatic ecosystems, microalgae are exposed to light fluctuations at different frequencies due to daily and seasonal changes. Although concentrations of herbicides are lower in Arctic than in temperate regions, atrazine and simazine, are increasingly found in northern aquatic systems because of long-distance aerial dispersal of widespread applications in the south and antifouling biocides used on ships. The toxic effects of atrazine on temperate microalgae are well documented, but very little is known about their effects on Arctic marine microalgae in relation to their temperate counterparts after light adaptation to variable light intensities. We therefore investigated the impacts of atrazine and simazine on photosynthetic activity, PSII energy fluxes, pigment content, photoprotective ability (NPQ), and reactive oxygen species (ROS) content under three light intensities. The goal was to better understand differences in physiological responses to light fluctuations between Arctic and temperate microalgae and to determine how these different characteristics affect their responses to herbicides. The Arctic diatom *Chaetoceros* showed stronger light adaptation capacity than the Arctic green algae *Micromonas*. Atrazine and simazine inhibited the growth and photosynthetic electron transport, affected the pigment content, and disturbed the energy balance between light absorption and utilization. As a result, during high light adaptation and in the presence of herbicides, photoprotective pigments were synthesized and NPQ was highly activated.

Nevertheless, these protective responses were insufficient to prevent oxidative damage caused by herbicides in both species from both regions, but at different extent depending on the species. Our study demonstrates that light is important in regulating herbicide toxicity in both Arctic and temperate microalgal strains. Moreover, eco-physiological differences in light responses are likely to support changes in the algal community, especially as the Arctic ocean becomes more polluted and bright with continued human impacts.

**Keywords:**

Marine microalgae, Atrazine, Simazine, Light, Photoadaptation, Ecotoxicology.

Abbreviations:

T-CN: Temperate *Chaetoceros neogracile*; T-MB; temperate *Micromonas bravo*; A-MP: Arctic *Micromonas polaris*; A-CN: Arctic *Chaetoceros neogracilis*; Car: carotenoids; Chl *a*: chlorophyll *a*; PSI: photosystem I; PSII: photosystem II; NPQ: non-photochemical quenching; qE: energy-dependent quenching; $Q_A$: primary electron acceptor of PSII; $Q_B$: secondary electron acceptor of PSII; RC: reaction center; $\Phi_M$: PSII maximum quantum yield; $\Phi'_M$: PSII operational quantum yield; ROS: reactive oxygen species; LL: low light intensity 40 µmol photons $m^{-2}$ $s^{-1}$, ML: medium light intensity 100 µmol photons $m^{-2}$ $s^{-1}$, HL: high light intensity 400 µmol photons $m^{-2}$ $s^{-1}$.

## Introduction

Light intensity is one of the most important environmental factors influencing the growth of photosynthetic organisms (Edwards et al. 2015). In aquatic environments, microalgae experience intense light fluctuations due to the daily sunlight exposure and seasonal variation (Wagner et al. 2006). Meanwhile, turbidity in the water and refraction of sunlight cause light intensity changes at different depths, with photon

flux scarcer in the deeper layers of the water column than at the surface (Dubinsky and Stambler 2009). To cope with the fluctuating light environments, photosynthetic organisms have evolved diverse phenotypic adjustments including photoadaptation processes (Deblois et al. 2013a, Handler 2017). Photoadaptation to low or high light environments involves changes at the gene level leading to modification of their physiology, biochemistry, and morphology (Bellacicco et al. 2016, Deblois et al. 2013b). Physiological photoprotection mechanisms of photosynthetic organisms include the PSII repair cycle, changes in pigment, de novo synthesis of proteins, state transitions, changes in energy efficiency transferred from the light-harvesting complex to reaction centers (RCs), and non-photochemical quenching (NPQ) induced by activation of the xanthophyll cycle (XC) (Deblois et al. 2013a, Dong et al. 2016, Hopes and Mock 2015). Among them, NPQ is the fastest and most flexible response to light variation (Goss and Lepetit 2015). In diatoms, the XC (de-epoxidation of diadinoxanthin to diatoxanthin) is activated by the light-driven acidification of the thylakoid lumen resulting in the accumulation of diatoxanthin. This process is a prerequisite for the formation of energy-dependent quenching (qE) that is the major component of NPQ in diatoms (Lepetit et al. 2017), which is not necessarily the case in plants and green algae (Allorent et al. 2013, Goss and Lepetit 2015).

As primary producers, microalgae constitute the basis of aquatic ecological trophic networks. The diatom *Chaetoceros sp.* and the small flagellate prasinophyte *Micromonas sp.* are dominant species in both Arctic and temperate regions (Balzano et al. 2012, Balzano et al. 2017, Seoane et al. 2019). They are thus among the non-target aquatic organisms exposed to pesticides (Chen et al. 2016). The effect of pesticides has been predominantly studied in freshwater ecosystems compared to marine and estuarine ecosystems (Dar et al. 2021, Dupraz et al. 2016). Herbicides are the most widely used among the major pesticide classes, and their toxic effects mainly affect the growth, photosynthesis, morphology, biochemical composition, and lipid content of microalgae (DeLorenzo 2001, Sun et al. 2020). The deleterious effects of specific photosystem II (PSII) inhibitor herbicides, such as atrazine and simazine, are

primarily to reduce photosynthetic efficiency by inhibiting photosynthetic electron transfer. It induces the production of reactive oxygen species (ROS) and further damage the D1 protein of PSII and biomolecules like pigments (Chalifour and Juneau 2011, Zhao et al. 2018). Some studies have shown that short-term light changes can affect the toxicity of pesticides (Baxter et al. 2016, Dong et al. 2016). However, very little is known about how photoadaptation to different light intensities influences the response of marine microalgae to herbicides.

Most of our knowledge regarding microalgal photoadaptation strategies and pesticide effects is from temperate species (Gomes and Juneau 2017, Young and Schmidt 2020). Microalgae have a rich evolutionary history due to their widespread presence in various habitats, especially marine ecosystems, leading to a wide range of adaptations, allowing them to thrive in a variety of environmental conditions (Lacour et al. 2020). Polar microalgae adapted to permanently low temperatures and extreme variation in irradiance due to seasonally changing ice-cover and day lengths (Handler 2017). Sea-ice of Arctic Ocean is gradually melting because of global warming, increasing light availability at the sea surface (Osborne et al. 2018). Therefore, studying the differences in the adaptation processes intrinsic to Arctic and temperate microalgae can provide insights into how microalgae will cope with the changing aquatic environment, including light intensity and herbicide presence. It is known that ice melting may potentially cause an increase in pesticide concentrations in the Arctic waters (Pućko et al. 2017), although at concentrations that will remain lower than the ones found in temperate regions. Indeed, the main source of pesticides in Arctic is from the long-range aerial transport and not the nearby agricultural activities as it is for temperate regions (Schmale et al. 2018, Vorkamp and Riget 2014). In this study, we aimed to determine the response to herbicides of Arctic and temperate microalgae photoadapted to various light intensities and how various photoadaptation strategies affect herbicide toxicity. Our comparison of eco-physiological responses of Arctic to their temperate counterparts will facilitate the development of population growth models for microalgae more generally, as models predicting microalgal biomass

changes due to light and contaminants generally use observations from only temperate algae.

## 2. Materials and methods

### 2.1 Algal species and growth conditions

Temperate *Chaetoceros neogracile* (T-CN-CCMP1425), temperate *Micromonas bravo* (T-MB-CCMP1646), and Arctic strain of *Micromonas polaris* (A-MP-CCMP2099) were purchased from NCMA (National Contract Management Association). The Arctic strain of *Chaetoceros neogracilis* (A-CN-RCC2279) was obtained from the Roscoff culture collection (France). All species were cultivated in L1 marine medium (Guillard and Hargraves 1993) with a total volume of 100 mL medium in 250 mL Erlenmeyer flasks. Microalgae were grown at three different light intensities under white fluorescent tubes (Philips F72T8/TL841/HO, New York, NY, USA) (low light intensity-40 µmol photons $m^{-2}$ $s^{-1}$ (LL), medium light intensity-100 µmol photons $m^{-2}$ $s^{-1}$ (ML), and high light intensity-400 µmol photons $m^{-2}$ $s^{-1}$ (HL)), intensities found at the surface of the Arctic Ocean and in temperate area (Lepetit et al. 2017, Leu et al. 2010), at 14:10 h (light: dark) illumination cycle and shaken moderately twice a day. Growth temperatures were 18 °C and 4 °C, respectively, for temperate and Arctic species. Cells were periodically transferred to fresh growth media to keep them in their exponential growth phase. The cells were cultured for more than ten generations in these growth conditions. The cell numbers were counted using Multisizer 3 Coulter Counter (Beckman Coulter Inc., USA). The calculation of growth rate (µ) is based on the following formula: $\mu = (\ln N_n) - (\ln N_0)/(t_n - t_0)$, where µ = average specific growth rate, $N_0$, $N_n$ indicate cell density (cells $mL^{-1}$) at respectively $t_0$ (beginning of the experiment) and $t_n$ (time, in days, after the beginning of the experiment).

### 2.2 Herbicide preparation and treatment

Atrazine and simazine used in this study came from Sigma-Aldrich (PESTANAL®, analytical standard, Canada). Herbicide stock solutions were made in pure acetone (≥ 99%) and acetone concentration was 0.01% in the treatments, which was verified not to be toxic to these microalgae. Six concentrations of atrazine and simazine were used for the herbicide tests (0 µg $L^{-1}$, 5 µg $L^{-1}$, 25 µg $L^{-1}$, 50 µg $L^{-1}$, 100 µg $L^{-1}$, and 250 µg $L^{-1}$). Cells were collected during their exponential growth phase and transferred to 1 L Erlenmeyer flasks (with 350 mL growth medium) at a cell density of $2.5 \times 10^5$ (*Chaetoceros*) and $2.5 \times 10^6$ (*Micromonas*) cells $mL^{-1}$ respectively, and then exposed to different concentrations of herbicides for 72 h under the three light conditions. Our experimental design follows standard procedure for toxicological tests with algae, the pH of the cultures did not change over the exposure period and all treatments were performed in triplicate. Cell density and cell biovolume were evaluated at the end of the experiment with a Multisizer 3 Coulter Counter particle analyzer (Beckman Coulter Inc., USA).

### 2.3 Pigment content measurement

Algal cultures (25 mL) were collected after 72 h herbicide treatment through a gentle filtration on 0.8µm filter membranes (Polytetrafluoroethylene; Xingya Purifyin Company; China). Filters were immediately submerged in liquid nitrogen and placed in 2 mL Eppendorf tubes, and then stored at -80 °C until analysis. Each sample was added to 2 mL of 90% acetone to be extracted overnight at -20 °C before pigment analysis. Cells in an ice container were broken for 20 s using an ultrasonic probe to increase extraction efficiency. The samples were centrifuged (10000×g) at 4 °C for 10 min after the extraction. The supernatants were used to quantify the content of chlorophyll (Chl *a*) and carotenoids (Car). A Cary 300 UV spectrophotometer (Varian, USA) was used to determine the absorbance spectra (400–750nm) for each extracted sample. Based on the equations from (Jeffrey and Humphrey 1975) and Seely et al. (1972), the contents of Chl *a* and Car were calculated respectively.

### 2.4 Variable Chl *a* fluorescence measurement

The samples (3 mL) were measured at their growth temperature of 4 °C and 18 °C after dark acclimation for 20 min. Fluorescence light curves performed with a fluorometer of Water-PAM (Walz, Germany) were used to evaluate the maximum ($\Phi_M$) and operational ($\Phi'_M$) PSII quantum yields, as well as the non-photochemical quenching (NPQ) (Du et al. 2019). The light curve was obtained by using eight levels of actinic light intensities (0, 46, 105, 188, 276, 427, 635, 906, and 1207 µmol photons $m^{-2}s^{-1}$) with saturation pulses (3000 µmol photons $m^{-2}$ $s^{-1}$, 800 ms). $\Phi_M$, $\Phi'_M$ and NPQ were computed according to the following equations: $\Phi_M = (F_M–F_0)/F_M$; $\Phi'_M = (F'_M–F_S)/F'_M$ (Genty et al. 1989); $NPQ = (F_M–F'_M)/F'_M$ (Bilger and Björkman 1990). Maximum relative electron transport rates ($rETR_{max}$), maximum light efficiency usage (α), and light saturation coefficient ($E_k$) were obtained by fitting the obtained values according to (Eilers and Peeters 1988, Serodio and Lavaud 2011). To further assess the PSII energy fluxes, the polyphasic increase in fluorescence transients was also captured by a PEA fluorometer (Plant Efficiency Analyzer, UK). The OJIP transients were generated by using a red light pulse of two seconds (3600 µmol photons $m^{-2}$ $s^{-1)}$ with a maximum emission at 650 nm (Jiang et al. 2008). Table S1 provides a description of each parameter.

## 2.5 Reactive oxygen species (ROS) measurement

Intracellular ROS content was determined by using a BD Accuri C6 flow cytometer (Biosciences, San Jose, CA, USA). The fluorescent dye $H_2$DCFDA (2′,7′-dichlorodihydrofluorescein diacetate, Molecular probes, Eugene, OR, USA) was used. More information about this method was described in (Stachowski-Haberkorn et al. 2013). Samples were analyzed after incubation in complete darkness for 30 min at room temperature. To prevent possible signal variations due to herbicide influence on FL1 fluorescence, the mean FL1 values of $H_2$DCFDA-stained samples were divided by the mean FL1 values of the same fresh samples analyzed for morphology. Results were thus expressed as FL1 ratios.

## 2.6 Atrazine determination

The concentration of atrazine removed from the growth medium was calculated by subtracting the concentration found in the sample (atrazine + growth medium + microalgae) treated for 72 h from the abiotic control (atrazine + growth medium). To measure atrazine concentration remaining in the growth medium i.e., removal capacity of microalgae, cultures (in triplicate) were transferred to 250 mL flasks containing 100 mL of L1 growth media at cell concentrations indicated in section 2.2 for 72 h. Abiotic controls, also in triplicate, were prepared using L1 medium without cells, and various light intensities did not alter the atrazine concentration. After inoculation of the microalgae in the medium, 2 mL aliquots of each flask were sampled and filtered on a 20 mm glass fiber filter (Type A/E, Pall Corporation, Michigan, USA) and stored in 1.5 mL Eppendorf tubes (polypropylene Safe-Lock tube, Canada). The filtrate was kept at -80 °C until analysis. After 72 h, the same procedure was repeated with 2 mL of culture for herbicide analysis. Before analysis, filtered media containing atrazine were thawed and then filtered again through a 0.22 µm syringe filter (Millex-GV, Millipore, Billerica, USA).

A stock solution of atrazine at 1 µg $L^{-1}$ was prepared in 50% methanol to perform a calibration curve ranging from 0.5-20 µg $L^{-1}$. An internal standard (IS) working solution of isotopically labeled atrazine-$d_5$ was prepared at 100 µg $L^{-1}$, 20 µL of which was added to each sample or standard with 180 µL. Quantitative analysis of atrazine was performed by QTRAP 5500 mass spectrometer (Sciex, Concord, ON, Canada) with a Turbo-V electrospray ionization source in positive ion multiple reaction monitoring (MRM) mode (Chalifour et al. 2016). Atrazine and IS were detected using MRM transitions *m/z* 216-174 and 221-179 for quantitation (at collision-offset voltage 30 and 25 V). Ion source and MS parameters were as follows: ESI voltage, 5000 V; source temperature, 500 °C; curtain gas, curtain gas, 35 psi; nebulizer and drying gases both at 50 psi. Peak integration was performed using Multiquant™ 3.0 (Sciex), using peak area ratios of analyte/IS and linear regression of calibration curve for quantitation.

2.7 Statistical analyses

Statistical analyses were performed using Origin® 7.0 (Originlab Corporation, Northampton, MA, USA). Two-way analysis of variance (ANOVA) was used to determine the effect of treatments, and Tukey's honestly significant difference (Tukey's, HSD) test was conducted to test the statistical significance of the differences between means of various treatments. The assumption of normal distribution and homogeneity of variances for all t-tests and ANOVAs presented were respectively tested using Lilliefors' and Levene's tests. Two-way analysis of variance (ANOVA) to evaluate the interactions between growth light conditions (LL, ML, and HL), and herbicide concentrations. Contrast analysis was used when there were significant differences in the studied variables between treatments. The $EC_{50}$ (half-maximum effective concentration) values were calculated from the nonlinear least-square fits by using the inverse of the regression curve (Juneau et al. 2001).

# 3. Results

## 3.1 Effects of the growth light intensity on the ecophysiological characteristics of the Arctic and temperate microalgae in absence of herbicides

### 3.1.1 Growth rate, cell biovolume, pigment content, and ROS content

Growth rates of Arctic and temperate microalgae (except for T-MB) grown under LL conditions were drastically lower than those under ML or HL conditions (Tukey's HSD, $P < 0.05$, Table 1, Fig. 1-atrazine concentration = 0 μg $L^{-1}$). Moreover, the growth rates of Arctic microalgae (*C. neogracilis*-A-CN and *M. polaris*-A-MP) were lower than their temperate counterparts (*C. neogracile*-T-CN, *M. bravo*-T-MB) under the three different light intensities; the exception being for A-CN under LL condition. In addition, the increasing trend of growth rate for Arctic microalgae was lower than that of temperate counterparts when the light intensity was enhanced. Similarly, the cell biovolume of two Arctic microalgae was smaller under LL condition compared to ML and HL (Tukey's HSD, $P < 0.05$, Table 1). Cell biovolume of the two temperate microalgae was the largest under HL and the smallest under LL, with an intermediary

biovolume for ML grown cultures.

The Chl *a* and Car contents of the two Arctic strains were lower than those of their temperate counterparts under LL, ML, and HL conditions. Furthermore, the Chl *a* content of the two temperate species significantly decreased under higher light intensities (ML, HL, Tukey's HSD, $P<0.05$, Fig. 2-atrazine concentration = 0 μg $L^{-1}$), while both Arctic species were unchanged under LL compared to ML and HL conditions. The Car content of the two temperate species increased significantly under high light intensity (ML and HL), while the two Arctic microalgae were not affected (Tukey's HSD, $P < 0.05$, Fig. 2). In addition, except for T-MB, we found higher ROS levels in microalgae grown under HL relative to the other two lower light conditions (LL and ML) (Fig. 3-atrazine concentration = 0 μg $L^{-1}$, Tukey's HSD, $P < 0.05$), and the ROS contents of T-CN, A-CN, and A-MP of HL grown cultures were 1.2, 2.3, and 1.4 times higher than those grown under LL, respectively.

3.1.2 Photosynthesis and energy dissipation processes

The maximum PSII quantum yield ($\Phi_M$) of all studied species significantly decreased with increasing growth light intensity and $\Phi_M$ of the two Arctic microalgae declined more than that of their temperate counterparts (Tukey's HSD, $P >0.05$, Table 1). A similar trend was observed with the operational PSII quantum yield ($\Phi'_M$), but the amplitudes of the declines were higher than for $\Phi_M$; except for A-MP showing no alteration from LL to ML (Table 1). Together with the reduction of $\Phi_M$ and $\Phi'_M$, the maximum light efficiency usage (α) showed a decreasing trend with increasing light intensity (Tukey's HSD, $P < 0.05$, Table 1). Furthermore, the maximum electron transport rates ($rETR_{max}$) and the light saturation coefficient ($E_k$) of Arctic and temperate diatoms (T-CN and A-CN) increased significantly from LL to ML (except for $E_k$ of T-CN) and remarkably decreased from ML to HL (Tukey's HSD, $P < 0.05$, Table 1). Under the same condition, the $E_k$ of Arctic and temperate green algae of *Micromonas* (T-MB and A-MP) demonstrated similar trends, but no significant difference (Tukey's HSD, $P >0.05$, Table 1). Moreover, the maximal ability for dissipation of excess energy ($NPQ_{max}$) of T-MB and A-MP also significantly increased

from LL to ML, and markedly decreased from ML to HL conditions (Tukey's HSD, $P < 0.05$, Table 1). However, the $NPQ_{max}$ of T-CN and A-CN increased significantly when the growth light intensity was high (LL to ML and HL, Tukey's HSD, $P < 0.05$, Table 1). In addition, we observed that the parameters $\Phi'_M$, $\Phi'_M$, α, $rETR_{max}$, and $E_k$ for the two Arctic species were, to different degrees, lower than those of their temperate counterparts under the different growth light intensities.

3.1.3 Photosystem II energy fluxes

The energy conservation parameter of $PI_{ABS}$ significantly decreased for all species, except for A-CN, with increasing the growth light intensity (Tukey's HSD, $P < 0.05$, Fig. 4). The $PI_{ABS}$ of the two Arctic microalgae was less affected than their temperate counterparts. The reduction in $PI_{ABS}$ was also reflected in the decrease of electron transport per active reaction center ($ET_0$/RC) for all studied species when the growth light intensity was enhanced. The effective dissipation per active RC ($DI_0$/RC) of the two temperate microalgae (T-CN and T-MB) was increased up to 252% and 224% from LL to HL (Tukey's HSD, $P < 0.05$). This was accompanied by an increase in the absorbed flux per active reaction center (ABS/RC) as an indicator of the PSII antenna size. In contrast, $DI_0$/RC and ABS/RC in two Arctic microalgae did not significantly change when the algae were grown under different light intensities (Tukey's HSD, $P > 0.05$, Fig. 4). The maximal rate at which excitons were trapped by the active RCs ($TR_0$/RC) was not affected by changes in growth light intensity. Furthermore, the PQ pool size participating in the electron transport (qPQ) and non-photochemical quenching ($qE_{max}$) were significantly increased in the two Arctic microalgae under HL, compared to ML and LL (Tukey's HSD, $P < 0.05$, Fig. 4). In contrast, the qPQ and $qE_{max}$ of the two temperate species significantly decreased with increasing light intensity.

## 3.2 Effects of atrazine and simazine on the ecophysiological characteristics of Arctic and temperate species

3.2.1 Growth rate, cell biovolume, pigment content, and ROS content

The growth rates of Arctic species (A-CN and A-MP) and their temperate counterparts (T-CN and T-MB) significantly decreased after 72 h exposure to atrazine or simazine independently of the growth light intensity (Tukey's HSD, $P < 0.05$, Fig. 1). Interestingly, although that trend was similar among the various light intensities, the effect was stronger under the lowest light intensity. Moreover, the impact of the herbicides on the growth rate for Arctic species was stronger than that of their temperate counterparts when light intensity was enhanced. Although these herbicides inhibited the growth of microalgae, the cell biovolume of the four studied species did not significantly change for any tested conditions (Tukey's HSD, $P>0.05$, Fig. S1), except for T-MB and A-MP at high concentrations (100 and 250 μg/L) under ML and HL conditions.

Chl *a* and Car contents did not change significantly at low concentrations of atrazine and simazine (≤ 25 μg/L, Tukey's HSD, $P > 0.05$, Fig. 2), but declined significantly at high concentrations (> 25μg/L). The maximum reduction was observed under HL compared to the other two low light intensities (LL and ML). Despite a decreasing trend in Chl *a* and Car, the ratio of Car/Chl *a* remained unchanged (Tukey's HSD, $P > 0.05$). ROS levels significantly increased with atrazine concentrations for each light condition (LL, ML, and HL) (Tukey's HSD, $P < 0.05$). Although this trend was similar among light intensities, the effect was stronger under HL (Fig. 3). The ROS content also significantly increased with increasing simazine concentrations, and its effect was greater for higher light intensities (data not shown).

**3.2.2** Photosynthesis and energy dissipation processes

The operational PSII quantum yield ($\Phi'_M$) of the four studied species significantly decreased (Tukey's HSD, $P < 0.05$, Fig. 5) with increasing atrazine and simazine concentrations for each growth light condition. Moreover, both $\Phi_M$ and $\Phi'_M$ of A-CN decreased more than that of T-CN. In contrast, $\Phi_M$ and $\Phi'_M$ of A-MP decreased less than that of T-MB except for low atrazine concentrations under LL (< 25 μg/L, Tukey's HSD, $P < 0.05$, Fig. 5). The evaluated $\Phi'_M$-$EC_{50}$ of T-CN for atrazine under LL, ML, and HL conditions were respectively 2.4, 1.7 and 1.8 times

higher than those obtained for A-CN (Table 1). Similar results were obtained for simazine. Both *Chaetoceros* species have the lowest $\Phi'_M$-$EC_{50}$ (respectively 90 µg $L^{-1}$ and 28 µg $L^{-1}$ for the temperate and Arctic species) for simazine under HL compared to LL and ML (Table 1). $\Phi'_M$-$EC_{50}$ of T-MB was equal to or higher than those of A-MP under LL, ML, and HL conditions for atrazine. The highest simazine $\Phi'_M$-$EC_{50}$ evaluated for A-MP under HL conditions (206 µg $L^{-1}$) was 4.2 times higher than that of T-MB (Table 1). The parameter of $\Phi'_M$ was more sensitive than $\Phi_M$ in response to the herbicides. The energy conservation parameter ($PI_{ABS}$) also decreased after exposure to 50 µg $L^{-1}$ atrazine and simazine under each light condition, but to a different extent than $\Phi_M$ and $\Phi'_M$ depending on the tested species (Table 2). Non-photochemical quenching ($qE_{max}$) of the four studied species was also significantly reduced with the addition of 50 µg $L^{-1}$ of atrazine under LL ML, and HL conditions (Tukey's HSD, $P < 0.05$, Table 2).

### 3.3 Effects of growth light intensity on atrazine toxicity

Because the effect of growth light intensity on simazine was similar to that of atrazine, and because atrazine is detected more frequently than simazine in water bodies, we mainly focus on atrazine for this section. Atrazine and ML alone significantly reduced $PI_{ABS}$ of T-CN by 98% and 95%, respectively, while their combined action was less effective (71% inhibition) (Tukey's HSD, $P < 0.05$). Similar results were observed for HL (Table 2). This trend was also observed among the other studied species (A-CN, T-MB, and A-MP). Both Arctic species increased their non-photochemical quenching ($qE_{max}$) to varying degrees (18-89%) under ML and HL growth conditions compared to LL (Table 2). The combined effect of atrazine and ML decreased $qE_{max}$ by 60% and 58% respectively in A-CN and A-MP (Table 2). Furthermore, the combined effect of atrazine and ML on the two temperate species only reduced $qE_{max}$ by 14% for T-MB and 63% for T-CN compared to ML exposure alone (27% and 72% reduction), and the combined effect of atrazine and HL decreased more $qE_{max}$ than the combination of atrazine and ML condition (Table 2). The treatment with atrazine alone significantly induced the production of ROS, but

the combined effect of atrazine and ML or HL downregulated the production of ROS (Table 2). According to Fig. 6, the removal of atrazine was stronger under high light growth (HL) compared to the other two low light intensities (LL and ML) except for T-CN (Tukey's HSD, $P < 0.05$). The removal ability of atrazine by A-CN was higher than that of T-CN under LL, ML and HL conditions. Meanwhile, the A-MP showed higher removal ability of atrazine compared to T-MB under ML and HL conditions except for LL condition.

# 4 Discussion

## 4.1 Influence of growth light intensity on Arctic microalgae and their temperate counterparts

### 4.1.1 Photoadaptation processes

Light adaptation processes developed by microalgae allow them to thrive in low or high light environments by modulating their eco-physiological properties (Agarwal et al. 2019, Young and Schmidt 2020). In our experiments, high light induced similar photophysiological responses among the studied species. Growth under higher (but not excessive) light intensity led to a significant increase in growth rates, which may be attributed to the Chl *a*/C evolution with changes in light intensity (Croteau et al. 2022, Lacour et al. 2018). The reduction of Chl *a* in all species after HL photoadaptation was typically seen as a result of lower light absorption as would be expected given that light absorption is positively related to cellular Chl *a* content (MacIntyre et al. 2002). Increase in Car may play a role in protecting the photosynthetic apparatus under high light intensities. Indeed, either directly or indirectly, these pigments are involved in scavenging ROS (Sedoud et al. 2014). Furthermore, the slight but significant increase of the light harvesting antenna size of all studied species following HL adaptation indicated a relatively low photochemically effective cross-section to reduce the chance of photons entering the photosynthetic electron transport chain to avoid photo-damage (Finkel et al. 2010).

These modifications observed under high light conditions minimized the excitation pressure on the photosynthetic apparatus despite the increased light availability (Agarwal et al. 2019). Non-photochemical quenching (NPQ) (the main component-qE) is known to be an efficient photoprotective mechanism (Goss and Lepetit 2015). The higher intrinsic $NPQ_{max}$ of the studied Arctic species under HL, as compared to LL and ML conditions, may indicate that this process is activated to reduce PSII damage (Kirilovsky 2015). Indeed, light intensity above the photosynthesis saturation point ($E_k$ over 400 µmol photons $m^{-2}$ $s^{-1}$, Table 1) can increase ROS production (Metsoviti et al. 2019), which was consistent with the reduced photosynthetic efficiency ($\Phi_M$ and $\Phi'_M$) under HL. Therefore, the observed high ROS content inducing inactivation of PSII under HL as compared to ML and LL, indicates that cellular defense strategies were not sufficient to deal with photochemical damage and oxidative stress.

### 4.1.2 Differences between Arctic and temperate microalgae

The observed low Chl *a* could be responsible for the lower photosynthetic efficiency ($\Phi_M$ and $\Phi'_M$) in both Arctic species compared to their temperate counterparts under all light conditions since Chl *a* is proportional to the number of photosynthetic systems (MacIntyre et al. 2002). Some authors have shown that the A-MP had only half the content of active PSII reaction centers compared to T-MB (Ni et al. 2017). This is also confirmed by the low performance index of photons ($PI_{ABS}$), showing the low photosynthetic efficiency. Furthermore, a small amount of Chl *a* is usually present in Arctic species growing under light-limiting conditions to avoid stacking effects between chlorophylls (Yan et al. 2018). As a result, the absence of markedly reduced Chl *a* content in HL-adapted Arctic cells compared with LL-adapted cells suggested that they did not possess the same light-modulating ability as temperate microalgae. Temperate microalgae usually decrease their light absorption at high irradiance levels by reducing Chl *a* associated with their light-harvesting complexes, as observed in both temperate species studied here (decreased Chl *a* under HL, Fig. 2). Interestingly, qPQ, which reflects the plastoquinone (PQ) pool size participating in the electron transport (Xu et al. 2019), significantly increased in the

two Arctic species under HL, indicating that increased electron supply to the PQ pool was satisfied by increasing the ability to transfer energy away from PSII, and accompanied by high dissipation capacity (higher $qE_{max}$) (Fig. 4). In comparison, temperate species had reduced qPQ and lower $qE_{max}$ under HL. The redox state of the PQ pool plays an important role in light adaptation of algae and regulation of gene expression in the chloroplasts and nucleus under varying light conditions (Lepetit et al. 2013, Virtanen et al. 2021). In summary, the photoadaptation strategies between temperate and Arctic microalgae show different extents. Arctic microalgae appear to mainly rely on increased PQ pool size and strong dissipation capacity ($qE_{max}$) to cope with higher light intensity, whereas their temperate counterparts appear to mainly rely on the reduction of pigments associated with light-harvesting complex (LHC) to regulate light absorption. In addition, we observed substantial differences in the adaptation capacity of the two microalgal classes. The diatoms had higher growth rate (μ), higher light efficiency use (α) and higher photosynthetic electron transfer rate ($rETR_{max}$) relative to the green microalgae, exhibiting their high photoadaptation capacity to change in ambient light intensity (Table 1). This mechanism concords with the dominance of diatoms in the seasonally changing Arctic Ocean (Croteau et al. 2022, Wolf et al. 2018).

### 4.2 Effects of atrazine and simazine on Arctic microalgae and their temperate counterparts under each light condition

Based on the $EC_{50}$ of $\Phi_M$ and $\Phi'_M$ (Table 1), temperate *C. neogracile* was more tolerant to atrazine and simazine than Arctic *C. neogracilis* under all light conditions, while Arctic *M. polaris* was less affected by these herbicides than temperate *M. bravo*, and the sensitivity sequence was T-CN<A-CN<A-MP<T-MP. We found that atrazine was more toxic than simazine in all studied species under all light conditions even though they had the same mode of action. This higher toxicity was attributed to the high log $K_{OW}$ of atrazine resulting in a high affinity for the herbicide binding site (Ronka 2016). Atrazine and simazine, as photosynthetic inhibitor herbicides, can bind to the $Q_B$ site of the D1 protein in PSII (Bai et al. 2015). Therefore, the observed

inhibition of photosynthetic electron transport chains (decreased $\Phi'_M$) in the Arctic and temperate species was observed in the presence of these herbicides, which was also evidenced by lower electron transfer per active RC ($ET_0$/RC). The transthylakoidal proton gradient required to activate non-photochemical quenching (qE) (Cao et al. 2013) was also reduced by inhibiting electron transport. As a result, the microalgae reduced thermal dissipation capacity ($qE_{max}$) under herbicide exposure preventing the efficient dissipation of excess energy. Therefore, the organisms underwent higher excitation pressure on PSII due to blocked electron transport, resulting in the production of large ROS concentrations (Fig. 3), which can eventually deactivate PSII RC (Gomes and Juneau 2017, Sun et al. 2020). This is in accordance with the increased effective antenna size of active RC (ABS/RC), showing a strong decrease in the active PSII RC population as previously demonstrated under cadmium and high light stress (Du et al. 2019). The reduction of active PSII RCs induced by ROS may explain the decreased photochemistry efficiency of PSII ($\Phi_M$), which was ultimately reflected in the growth inhibition of all studied species under the different light conditions. This observation was consistent with previous studies showing that photosynthesis inhibitor herbicides (diuron and Irgarol) inhibit the growth of freshwater microalgae (Kottuparambil et al. 2017). In addition, the reduction of Chl *a* in all species (Fig. 2) was attributed to the continuous accumulation of ROS in the presence of atrazine or simazine (Almeida et al. 2017). Atrazine and simazine disturbed the balance between light absorption and energy utilization, since $PI_{ABS}$, as an indicator for energy conservation from photons absorbed by PSII to intersystem electron acceptors, significantly decreased irrespective of growth light intensity (Sun et al. 2020).

### 4.3 Combined effects of growth light intensity and atrazine on Arctic microalgae and their temperate counterparts

Significant interactions between growth light intensity and atrazine were observed for growth, $\Phi_M$, $\Phi'_M$, and $PI_{ABS}$ ($P<0.0001$). Atrazine was chosen to describe the interaction with light since the obtained results for simazine were similar due to

their same mode of action. According to the $EC_{50}$ of $\Phi_M$ and $\Phi'_M$, all studied species were more affected by atrazine under HL compared to the other lower light intensities (LL and ML) (Table 1). Although atrazine and light alone, respectively, decreased the light energy conversion ($PI_{ABS}$), interestingly it appears that the combination of HL and herbicides reversed this effect on $PI_{ABS}$ (Table 2). This indicates that photoadaptation processes, such as changes in pigments, mitigate the effects of herbicides on light energy conversation. Indeed, lower Chl *a* in both Arctic species and higher Car concentration in both temperate species may decrease, respectively, light absorption and ROS scavenging, which help to protect the photosystem apparatus. The combined inhibitory effect was small in tolerant species (T-CN and A-MP) to atrazine compared to the sensitive species (A-CN and T-MB). Changes in PSII photochemistry are frequently related to the modifications of the energy dissipation pathway ($qE_{max}$) (Du et al. 2019). The combined effect of HL and atrazine (50 µg $L^{-1}$, concentration near the $EC_{50}$ for most species) on the thermal dissipation ability ($qE_{max}$) of Arctic species was greater than the effects of atrazine alone, although high $qE_{max}$ was already induced after HL adaptation without herbicide. While the effect of $qE_{max}$ was slight in temperate species under the combined conditions of HL and atrazine, HL and atrazine alone considerably decreased $qE_{max}$ (Table 2). Therefore, we can suggest that other parts of the non-photochemical energy dissipation process (qT or qI) in temperate species were highly effective under HL adaptation since some authors have shown that qE was in general much lower on green microalgae than in diatoms since qT is more important than qE in green algae of *Chlamydomonas* (Allorent et al. 2013). These results showed that $qE_{max}$, as an indicator of the thermal dissipation capacity, was less indicative than $\Phi'_M$ and $PI_{ABS}$, probably because the later integrated the effects of the herbicide and HL on the photosynthetic electron transport and the related energy dissipation processes, while $qE_{max}$ only represents one of the components of NPQ. This is in accordance with a recent study showing that the performance index $PI_{ABS}$ was a more convincing indicator of atrazine toxicity compared to growth rate and $\Phi_{E0}$ (Sun et al. 2020). On the other hand, the combination of HL effect and 50 µg $L^{-1}$ atrazine of microalgae mitigated the ROS

burst (Table 2), which was attributed to the increased non-photochemical quenching ($NPQ_{max}$) after HL adaptation to dissipate excess energy to reduce the excitation pressure on PSII (Silva et al. 2021). Furthermore, with the exception of T-CN, the removal of atrazine by microalgae increased with increasing culture light intensity (LL-ML-HL), which can largely explain the high herbicide toxicity under HL intensity. We hypothesize that high light condition induces higher uptake of pesticides as it was previously demonstrated for other contaminants such as metals (Du et al. 2019). As a result, we can assume that even the effective induction of photosynthetic defense measures (NPQ and Car content) upon HL adaptation was unable to deal with the combination of higher light intensity and herbicides. Interestingly, the growth inhibition caused by atrazine of temperate species grown under HL was alleviated more than the cells grown under LL and ML (Fig. 1). This can be explained that temperate microalgae can effectively utilize the absorbed light energy and perform reasonable energy allocation (high α and $PI_{ABS,}$ Table 1) for carbon fixation. However, Arctic microalgae grown under HL were unable to prevent growth inhibition caused by atrazine due to the observed inefficient capacity for light absorption and light energy conversion (Fig. 4).

### 4.4 Concluding remarks

We demonstrated that the extent of light-adaption responses between Arctic and temperate microalgae were different, these differences can influence the toxicity of atrazine, and probably other contaminants. Furthermore, the microalgal protection measures of NPQ and Car (photoprotective pigment) after HL adaptation were insufficient to handle the combined impacts of high light intensity and atrazine stress, as atrazine removal ability was enhanced with increasing growth light intensity. Our results indicated that light plays a non-negligible role in regulating the toxicity of herbicide for microalgae. We recommend that variation in light intensities should be considered in herbicide risk assessments for Arctic and temperate ecosystems, because of its role in affecting photoprotective strategies and atrazine removal.

### Acknowledgments

This work was supported by a DFO grant (MECTS-#3789712) obtained by Philippe Juneau, Johann Lavaud, and Beatrix Beisner, and the Natural Science and Engineering Research Council of Canada (NSERC) (RGPIN-2017-06210) awarded to Philippe Juneau. The authors thanks also the GRIL (Groupe de recherche interuniversitaire en limnologie) for funding to PJ and BEB that supported Juan Du's Ph.D.

# References


Agarwal, A., Patil, S., Gharat, K., Pandit, R.A. and Lali, A.M. (2019) Modulation in light utilization by a microalga *Asteracys* sp. under mixotrophic growth regimes. Photosynthesis Research 139(1-3), 553-567.

Allorent, G., Tokutsu, R., Roach, T., Peers, G., Cardol, P., Girard-Bascou, J., Seigneurin-Berny, D., Petroutsos, D., Kuntz, M., Breyton, C., Franck, F., Wollman, F.A., Niyogi, K.K., Krieger-Liszkay, A., Minagawa, J. and Finazzi, G. (2013) A dual strategy to cope with high light in *Chlamydomonas reinhardtii*. Plant Cell 25(2), 545-557.

Almeida, A.C., Gomes, T., Langford, K., Thomas, K.V. and Tollefsen, K.E. (2017) Oxidative stress in the algae *Chlamydomonas reinhardtii* exposed to biocides. Aquatic Toxicology 189, 50-59.

Bai, X., Sun, C., Xie, J., Song, H., Zhu, Q., Su, Y., Qian, H. and Fu, Z. (2015) Effects of atrazine on photosynthesis and defense response and the underlying mechanisms in *Phaeodactylum tricornutum*. Environmental Science and Pollution Research 22(17), 499-507.

Balzano, S., Marie, D., Gourvil, P. and Vaulot, D. (2012) Composition of the summer photosynthetic pico and nanoplankton communities in the Beaufort Sea assessed by T-RFLP and sequences of the 18S rRNA gene from flow cytometry sorted samples. ISME Journal 6(8), 1480-1498.

Balzano, S., Percopo, I., Siano, R., Gourvil, P., Chanoine, M., Marie, D., Vaulot, D. and Sarno, D. (2017) Morphological and genetic diversity of Beaufort Sea diatoms with high contributions from the Chaetoceros neogracilis species complex. J Phycol 53(1), 161-187.

Baxter, L., Brain, R.A., Lissemore, L., Solomon, K.R., Hanson, M.L. and Prosser, R.S. (2016) Influence of light, nutrients, and temperature on the toxicity of atrazine to the algal species *Raphidocelis subcapitata*: Implications for the risk assessment of herbicides. Ecotoxicology and Environmental Safety 132, 250-259.

Bellacicco, M., Volpe, G., Colella, S., Pitarch, J. and Santoleri, R. (2016) Influence of photoacclimation on the phytoplankton seasonal cycle in the Mediterranean Sea as seen by satellite. Remote Sensing of Environment 184, 595-604.

Bilger, W. and Björkman, O. (1990) Role of the xanthophyll cycle in photoprotection elucidated by measurements of light-induced absorbance changes, fluorescence and photosynthesis in leaves of *Hedera canariensis*. Photosynthesis Research 25(3), 173-185.

Cao, S., Zhang, X., Xu, D., Fan, X., Mou, S., Wang, Y., Ye, N. and Wang, W. (2013) A transthylakoid proton gradient and inhibitors induce a non-photochemical fluorescence quenching in unicellular algae Nannochloropsis sp. FEBS Letters 587(9), 1310-1315.

Chalifour, A. and Juneau, P. (2011) Temperature-dependent sensitivity of growth and photosynthesis of *Scenedesmus obliquus*, *Navicula pelliculosa* and two strains of *Microcystis aeruginosa* to the herbicide atrazine. Aquatic Toxicology 103(1-2), 9-17.

Chalifour, A., LeBlanc, A., Sleno, L. and Juneau, P. (2016) Sensitivity of

*Scenedesmus obliquus* and *Microcystis aeruginosa* to atrazine: effects of acclimation and mixed cultures, and their removal ability. Ecotoxicology 25(10), 1822-1831.
Chen, S., Chen, M., Wang, Z., Qiu, W., Wang, J., Shen, Y., Wang, Y. and Ge, S. (2016) Toxicological effects of chlorpyrifos on growth, enzyme activity and chlorophyll a synthesis of freshwater microalgae. Environmental Toxicology Pharmacology 45, 179-186.
Croteau, D., Lacour, T., Schiffrine, N., Morin, P.I., Forget, M.H., Bruyant, F., Ferland, J., Lafond, A., Campbell, D.A., Tremblay, J.É., Babin, M. and Lavaud, J. (2022) Shifts in growth light optima among diatom species support their succession during the spring bloom in the Arctic. Journal of Ecology.
Dar, G.H., Hakeem, K.R., Mehmood, M.A. and Qadri, H. (2021) Freshwater Pollution and Aquatic Ecosystems: Environmental Impact and Sustainable Management. CRC Press.
Deblois, C.P., Dufresne, K. and Juneau, P. (2013a) Response to variable light intensity in photoacclimated algae and cyanobacteria exposed to atrazine. Aquatic Toxicology 126, 77-84.
Deblois, C.P., Marchand, A. and Juneau, P. (2013b) Comparison of photoacclimation in twelve freshwater photoautotrophs (chlorophyte, bacillaryophyte, cryptophyte and cyanophyte) isolated from a natural community. PLoS One 8(3), e57139.
DeLorenzo, M.E. (2001) toxicity of pesticides to aquatic microorganisms: a review. Environmental Toxicology and Chemistry 20 (1), 84-98.
Dong, H.P., Dong, Y.L., Cui, L., Balamurugan, S., Gao, J., Lu, S.H. and Jiang, T. (2016) High light stress triggers distinct proteomic responses in the marine diatom *Thalassiosira pseudonana*. BMC Genomics 17(1), 994.
Du, J., Qiu, B., Pedrosa Gomes, M., Juneau, P. and Dai, G. (2019) Influence of light intensity on cadmium uptake and toxicity in the cyanobacteria *Synechocystis* sp. PCC6803. Aquatic Toxicology 211, 163-172.
Dubinsky, Z. and Stambler, N. (2009) Photoacclimation processes in phytoplankton: mechanisms, consequences, and applications. Aquatic Microbial Ecology 56, 163-176.
Dupraz, V., Coquille, N., Menard, D., Sussarellu, R., Haugarreau, L. and Stachowski-Haberkorn, S. (2016) Microalgal sensitivity varies between a diuron-resistant strain and two wild strains when exposed to diuron and irgarol, alone and in mixtures. Chemosphere 151, 241-252.
Edwards, K.F., Thomas, M.K., Klausmeier, C.A. and Litchman, E. (2015) Light and growth in marine phytoplankton: allometric, taxonomic, and environmental variation. Limnology and Oceanography 60(2), 540-552.
Eilers, P.H.C. and Peeters, J.C.H. (1988) A model for the relationship between light intensity and the rate of photosynthesis in phytoplankton. Ecological Modelling 42(3-4), 199-215.
Finkel, Z.V., Beardall, J., Flynn, K.J., Quigg, A., Rees, T.A.V. and Raven, J.A. (2010) Phytoplankton in a changing world: cell size and elemental stoichiometry. Journal of Plankton Research 32(1), 119-137.
Genty, B., Briantais, J.M. and Baker, N.R. (1989) The relationship between the quantum yield of photosynthetic electron transport and quenching of chlorophyll

fluorescence. Biochimica et Biophysica Acta 990(1), 87-92.
Gomes, M.P. and Juneau, P. (2017) Temperature and Light Modulation of Herbicide Toxicity on Algal and Cyanobacterial Physiology. Frontiers in Environmental Science 5.
Goss, R. and Lepetit, B. (2015) Biodiversity of NPQ. Journal of Plant Physiology 172, 13-32.
Guillard, R.R.L. and Hargraves, P.E. (1993) *Stichochrysis immobilis* is a diatom, not a chrysophyte. Phycologia 32(3), 234-236.
Handler, E. (2017) Responses to Light Intensity and Regimes by an Arctic strain of the picophytoplankton *Micromonas* CCMP2099.
Hopes, A. and Mock, T. (2015) eLS, pp. 1-9.
Jeffrey, S.W. and Humphrey, G.F. (1975) New spectrophotometric equations for determining chlorophylls a, b, c1 and c2 in higher plants, algae and natural phytoplankton. Biochemie und Physiologie der Pflanzen 167(2), 191-194.
Jiang, H.X., Chen, L.S., Zheng, J.G., Han, S., Tang, N. and Smith, B.R. (2008) Aluminum-induced effects on Photosystem II photochemistry in Citrus leaves assessed by the chlorophyll a fluorescence transient. Tree Physiology 28(12), 1863-1871.
Juneau, P., David, D. and Saburo, M. (2001) Evaluation of different algal species sensitivity to mercury and metolachlor by PAM-fluorometry. Chemosphere 45(4-5), 589-598.
Kirilovsky, D. (2015) Modulating energy arriving at photochemical reaction centers: orange carotenoid protein-related photoprotection and state transitions. Photosynthesis Research 126(1), 3-17.
Kottuparambil, S., Brown, M.T., Park, J., Choi, S., Lee, H., Choi, H.G., Depuydt, S. and Han, T. (2017) Comparative assessment of single and joint effects of diuron and Irgarol 1051 on Arctic and temperate microalgae using chlorophyll a fluorescence imaging. Ecological Indicators 76, 304-316.
Lacour, T., Babin, M. and Lavaud, J. (2020) Diversity in xanthophyll cycle pigments content and related nonphotochemical quenching (NPQ) among microalgae: implications for growth strategy and ecology. Journal of Phycology 56(2), 245-263.
Lacour, T., Larivière, J., Ferland, J., Bruyant, F., Lavaud, J. and Babin, M. (2018) The Role of Sustained Photoprotective Non-photochemical Quenching in Low Temperature and High Light Acclimation in the Bloom-Forming Arctic Diatom *Thalassiosira gravida*. Frontiers in Marine Science 5.
Lepetit, B., Gelin, G., Lepetit, M., Sturm, S., Vugrinec, S., Rogato, A., Kroth, P.G., Falciatore, A. and Lavaud, J. (2017) The diatom *Phaeodactylum tricornutum* adjusts nonphotochemical fluorescence quenching capacity in response to dynamic light via fine-tuned Lhcx and xanthophyll cycle pigment synthesis. New Phytologist 214(1), 205-218.
Lepetit, B., Sturm, S., Rogato, A., Gruber, A., Sachse, M., Falciatore, A., Kroth, P.G. and Lavaud, J. (2013) High light acclimation in the secondary plastids containing diatom *Phaeodactylum tricornutum* is triggered by the redox state of the plastoquinone pool. Plant physiology 161(2), 853-865.

Leu, E., Wiktor, J., Søreide, J.E., Berge, J. and Falk-Petersen, S. (2010) Increased irradiance reduces food quality of sea ice algae. Marine Ecology Progress Series 411, 49-60.
MacIntyre, H.L., Todd, M.K. and Todd, H.K. (2002) PHOTOACCLIMATION OF PHOTOSYNTHESIS IRRADIANCE RESPONSE CURVES AND PHOTOSYNTHETIC. Journal of Phycology.
Metsoviti, M.N., Papapolymerou, G., Karapanagiotidis, I.T. and Katsoulas, N. (2019) Effect of Light Intensity and Quality on Growth Rate and Composition of *Chlorella vulgaris*. Plants (Basel) 9(1).
Ni, G., Zimbalatti, G., Murphy, C.D., Barnett, A.B., Arsenault, C.M., Li, G., Cockshutt, A.M. and Campbell, D.A. (2017) Arctic *Micromonas* uses protein pools and non-photochemical quenching to cope with temperature restrictions on Photosystem II protein turnover. Photosynthesis Research 131(2), 203-220.
Osborne, E., Richter-Menge, J. and Jeffries, M. (2018) Tundra greenness. Arctic Report Card, 2018.
Pućko, M., Stern, G.A., Burt, A.E., Jantunen, L.M., Bidleman, T.F., Macdonald, R.W., Barber, D.G., Geilfus, N.X. and Rysgaard, S. (2017) Current use pesticide and legacy organochlorine pesticide dynamics at the ocean-sea ice-atmosphere interface in resolute passage, Canadian Arctic, during winter-summer transition. Science of the Total Environment 580, 1460-1469.
Ronka, S. (2016) Removal of triazine-based herbicides on specific polymeric sorbent: batch studies. Pure and Applied Chemistry 88(12), 1167-1177.
Schmale, J., Arnold, S.R., Law, K.S., Thorp, T., Anenberg, S., Simpson, W.R., Mao, J. and Pratt, K.A. (2018) Local Arctic Air Pollution: A Neglected but Serious Problem. Earth's Future 6(10), 1385-1412.
Sedoud, A., Lopez-Igual, R., Ur Rehman, A., Wilson, A., Perreau, F., Boulay, C., Vass, I., Krieger-Liszkay, A. and Kirilovsky, D. (2014) The Cyanobacterial Photoactive Orange Carotenoid Protein Is an Excellent Singlet Oxygen Quencher. Plant Cell 26(4), 1781-1791.
Seoane, M., Gonzalez-Fernandez, C., Soudant, P., Huvet, A., Esperanza, M., Cid, A. and Paul-Pont, I. (2019) Polystyrene microbeads modulate the energy metabolism of the marine diatom Chaetoceros neogracile. Environ Pollut 251, 363-371.
Serodio, J. and Lavaud, J. (2011) A model for describing the light response of the nonphotochemical quenching of chlorophyll fluorescence. Photosynthesis Research 108(1), 61-76.
Silva, F.B., Costa, A.C., Megguer, C.A., Lima, J.S., Batista, P.F., Martins, D.A., Almeida, G.M., Domingos, M. and Müller, C. (2021) Atrazine toxicity to handroanthus heptaphyllus, a nontarget species from a Brazilian biome threatened by agriculture. Environmental Quality Management 30(3), 17-25.
Stachowski-Haberkorn, S., Jerome, M., Rouxel, J., Khelifi, C., Rince, M. and Burgeot, T. (2013) Multigenerational exposure of the microalga *Tetraselmis suecica* to diuron leads to spontaneous long-term strain adaptation. Aquatic Toxicology 140-141, 380-388.
Sun, C., Xu, Y., Hu, N., Ma, J., Sun, S., Cao, W., Klobucar, G., Hu, C. and Zhao, Y.

(2020) To evaluate the toxicity of atrazine on the freshwater microalgae *Chlorella* sp. using sensitive indices indicated by photosynthetic parameters. Chemosphere 244, 125514.

Virtanen, O., Khorobrykh, S. and Tyystjarvi, E. (2021) Acclimation of *Chlamydomonas reinhardtii* to extremely strong light. Photosynthesis Research 147(1), 91-106.

Vorkamp, K. and Riget, F.F. (2014) A review of new and current-use contaminants in the Arctic environment: evidence of long-range transport and indications of bioaccumulation. Chemosphere 111, 379-395.

Wagner, H., Jakob, T. and Wilhelm, C. (2006) Balancing the energy flow from captured light to biomass under fluctuating light conditions. New Phytologist 169(1), 95-108.

Wolf, K.K.E., Hoppe, C.J.M. and Rost, B. (2018) Resilience by diversity: Large intraspecific differences in climate change responses of an Arctic diatom. Limnology and Oceanography 63(1), 397-411.

Xu, K., Racine, F., He, Z. and Juneau, P. (2019) Impacts of hydroxyphenylpyruvate dioxygenase (HPPD) inhibitor (mesotrione) on photosynthetic processes in *Chlamydomonas reinhardtii*. Environmental Pollution 244, 295-303.

Yan, D., Beardall, J. and Gao, K. (2018) Variation in cell size of the diatom *Coscinodiscus granii* influences photosynthetic performance and growth. Photosynthesis Research 137(1), 41-52.

Young, J.N. and Schmidt, K. (2020) It's what's inside that matters: physiological adaptations of high-latitude marine microalgae to environmental change. New Phytologist 227(5), 1307-1318.

Zhao, F., Li, Y., Huang, L., Gu, Y., Zhang, H., Zeng, D. and Tan, H. (2018) Individual and combined toxicity of atrazine, butachlor, halosulfuron-methyl and mesotrione on the microalga *Selenastrum capricornutum*. Ecotoxicology and Environmental Safety 148, 969-975.

Table 1. The effect of light intensity (LL, ML, and HL) on the growth rate, cell biovolume, $\Phi_M$, $\Phi'_M$, α, $rETR_{max}$, $E_k$, and $NPQ_{max}$ of temperate *C. neogracile* (T-CN), *M. bravo* (T-MB), Arctic *C. neogracilis* (A-CN), and Arctic *M. polaris* (A-MP). $EC_{50}$ for the operational PSII quantum yield ($\Phi'_M$) after 72 h exposure to atrazine and simazine under three different light intensities (LL, ML, and HL). Strains in the same column exposed to the different light intensity with different superscript letters (a-c) were significantly different (Tukey's HSD, $P < 0.05$). The numbers in parentheses are the percentages of the control values. Data expressed as means ± SD (n = 6).

795

| Species | Light | Growth rate ($\mu$) | Volume ($\mu m^3$) | $\Phi_M$ | $\Phi'_M$ | $\alpha$ | $rETR_{max}$ | $E_k$ | $NPQ_{max}$ | $EC_{50}$-$\Phi'_M$ (Atra) | $EC_{50}$-$\Phi'_M$ (Sim) |
|---|---|---|---|---|---|---|---|---|---|---|---|
| T-CN | LL | 0.37±0.02 (100)$^{a}$ | 114±8.89(100)$^{a}$ | 0.692±0.00 (100)$^{a}$ | 0.682±0.01 (100)$^{a}$ | 0.713±0.01 (100)$^{a}$ | 333±36 (100)$^{a}$ | 467±52 (100)$^{a}$ | 1.5±1.24 (100)$^{a}$ | 95±7.4 | 121±7.9 |
| | ML | 0.64±0.03 (170)$^{b}$ | 148±9.59(130)$^{b}$ | 0.647±0.00 (93)$^{b}$ | 0.646±0.00 (95)$^{b}$ | 0.665±0.01 (93)$^{b}$ | 421±17 (126)$^{b}$ | 633±23 (136)$^{b}$ | 1.3±0.24 (12)$^{b}$ | 66±1.4 | 142±6.7 |
| | HL | 0.66±0.02 (177)$^{b}$ | 164±4.88(144)$^{c}$ | 0.608±0.01 (88)$^{c}$ | 0.510±0.03 (75)$^{c}$ | 0.624±0.02 (88)$^{c}$ | 253±63 (76)$^{c}$ | 404±91 (87)$^{a}$ | 10±0.00 (105)$^{a}$ | 34±1.1 | 90±12 |
| A-CN | LL | 0.43±0.03 (100)$^{a}$ | 45±3.06 (100)$^{a}$ | 0.674±0.01 (100)$^{a}$ | 0.607±0.01 (100)$^{a}$ | 0.607±0.02 (100)$^{a}$ | 265±34 (100)$^{a}$ | 432±55 (100)$^{a}$ | 1.6±0.62 (100)$^{a}$ | 39±1.7 | 52±0.7 |
| | ML | 0.57±0.09 (131)$^{b}$ | 63±3.84 (140)$^{b}$ | 0.584±0.00 (87)$^{b}$ | 0.553±0.01 (91)$^{b}$ | 0.569±0.04 (94)$^{a}$ | 370±91 (140)$^{b}$ | 648±158 (150)$^{b}$ | 1.8±0.54 (113)$^{a}$ | 37±2.1 | 62±2.1 |
| | HL | 0.57±0.08 (130)$^{b}$ | 61±7.57 (136)$^{b}$ | 0.525±0.02 (78)$^{c}$ | 0.246±0.02 (41)$^{c}$ | 0.473±0.07 (78)$^{b}$ | 91±13 (34)$^{c}$ | 196±46 (45)$^{c}$ | 3.7±0.92 (231)$^{b}$ | 12±3.2 | 28±2.0 |
| T-MB | LL | 0.36±0.01 (100)$^{a}$ | 4±0.09 (100)$^{a}$ | 0.685±0.01 (100)$^{a}$ | 0.678±0.02 (100)$^{a}$ | 0.519±0.05 (100)$^{ab}$ | 247±61 (100)$^{a}$ | 369±162 (100)$^{a}$ | 1.5±0.01 (100)$^{a}$ | 36±5.9 | 61±7.0 |
| | ML | 0.58±0.03 (160)$^{b}$ | 5±0.00 (134)$^{b}$ | 0.647±0.00 (94)$^{b}$ | 0.562±0.00 (83)$^{b}$ | 0.597±0.01 (115)$^{a}$ | 244±25 (99)$^{a}$ | 430±48 (117)$^{a}$ | 1.9±0.11 (127)$^{b}$ | 31±2.3 | 32±1.8 |
| | HL | 0.80±0.05 (220)$^{c}$ | 5±0.19 (141)$^{c}$ | 0.598±0.01 (87)$^{c}$ | 0.357±0.01 (53)$^{c}$ | 0.499±0.07 (96)$^{b}$ | 180±31 (73)$^{a}$ | 368±82 (100)$^{a}$ | 1.3±0.33 (87)$^{a}$ | 30±4.8 | 49±1.4 |
| A-MP | LL | 0.27±0.01 (100)$^{a}$ | 5±0.05 (100)$^{a}$ | 0.675±0.02 (100)$^{a}$ | 0.505±0.02 (100)$^{a}$ | 0.445±0.09 (100)$^{ab}$ | 114±56 (100)$^{a}$ | 249±104 (100)$^{a}$ | 2.2±0.71 (100)$^{a}$ | 39±1.3 | 55±3.4 |
| | ML | 0.30±0.02 (109)$^{b}$ | 6±0.26 (102)$^{a}$ | 0.618±0.02 (92)$^{b}$ | 0.491±0.02 (97)$^{a}$ | 0.493±0.04 (111)$^{a}$ | 156±21 (137)$^{a}$ | 356±28 (143)$^{a}$ | 9.8±0.37 (445)$^{b}$ | 36±1.7 | 46±1.9 |
| | HL | 0.32±0.04 (118)$^{b}$ | 6±0.10 (114)$^{b}$ | 0.515±0.00 (76)$^{c}$ | 0.222±0.01 (44)$^{b}$ | 0.384±0.04 (86)$^{b}$ | 106±54 (93)$^{a}$ | 273±128 (110)$^{a}$ | 1.6±0.20 (73)$^{a}$ | 29±0.6 | 206±39 |

796

797 Table 2. Effect of atrazine (50 μg $L^{-1}$), ML & HL exposure and the combined effect (light and atrazine) on
798 light energy conservation indicator ($PI_{ABS}$), non-photochemical quenching ($qE_{max}$), and ROS content, in
799 percentage from control (control is taken as 100%). Data are means ± SD of two independent experiments in
800 triplicate. Within treatments, values followed by one asterisk are significantly different from the control, and
801 values followed by two asterisks indicate significant differences between the LL and ML or HL exposure,
802 while values followed by three asterisks are significantly different from both control and ML and HL
803 treatment (Tukey's HSD, $P < 0.05$).

| Species | Parameter | Effect of atrazine % of the control (±) LL | Effect of ML % of the control (±) | Atrazine+ ML % of the control (±) | Effect of HL % of the control (±) | Atrazine+ HL % of the control (±) |
|---|---|---|---|---|---|---|
| T-CN | $PI_{ABS}$ | 2* (0) | 5** (0) | 29*,** (2) | 5** (0) | 21*,** (1) |
| A-CN | $PI_{ABS}$ | 37* (2) | 75** (5) | 16*,** (1) | 57** (1) | 11*,** (1) |
| T-MB | $PI_{ABS}$ | 52* (2) | 4** (0) | 5*,** (0) | 3** (0) | 8*,** (0) |
| A-MP | $PI_{ABS}$ | 10* (1) | 48** (2) | 28*,** (2) | 40** (2) | 15 (1) |
| T-CN | qEmax | 85* (9) | 28** (2) | 37*,** (1) | 26** (2) | 24*,** (2) |
| A-CN | qEmax | 78* (3) | 118 (16) | 40*,** (2) | 124** (15) | 28*,** (3) |
| T-MB | qEmax | 97 (5) | 73** (6) | 86 (5) | 66** (3) | 70*,** (7) |
| A-MP | qEmax | 81* (3) | 183** (24) | 42*,** (3) | 189** (19) | 23*,** (2) |
| T-CN | ROS | 171* (12) | 101 (10) | 131*,** (14) | 114 (10) | 138*,** (21) |
| A-CN | ROS | 243* (18) | 163** (21) | 466*,** (42) | 227** (32) | 286*,** (25) |
| T-MB | ROS | 444* (72) | 107 (7) | 162*,** (12) | 116 (17) | 231*,** (18) |
| A-MP | ROS | 176* (12) | 105 (8) | 113*,** (17) | 36** (4) | 390*,** (47) |

804

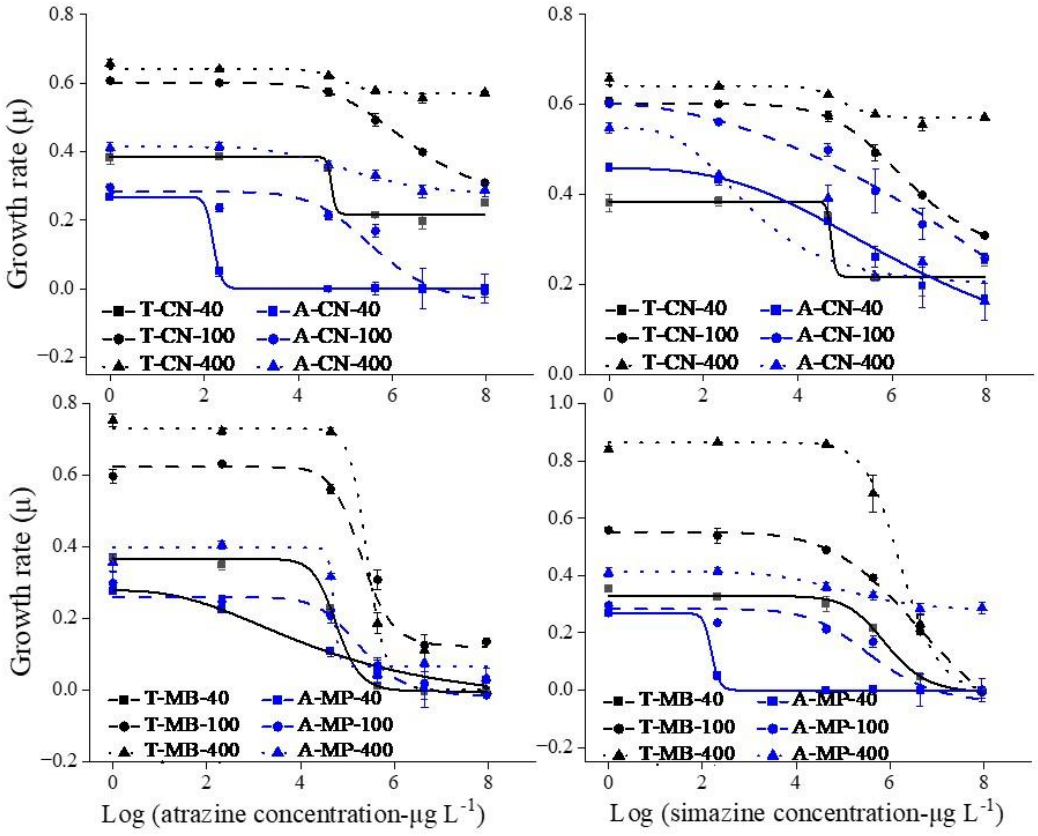


Figure 1. The effect of atrazine and simazine on the growth rate of four species (temperate *C. neogracile* (T-CN), Arctic *C. neogracilis* (A-CN), temperate *M. bravo* (T-MB), and Arctic *M. polaris* (A-MP)) after 72 h exposure under LL (square), ML (circle) and HL (triangle). Data expressed as means ± SD (n = 6)

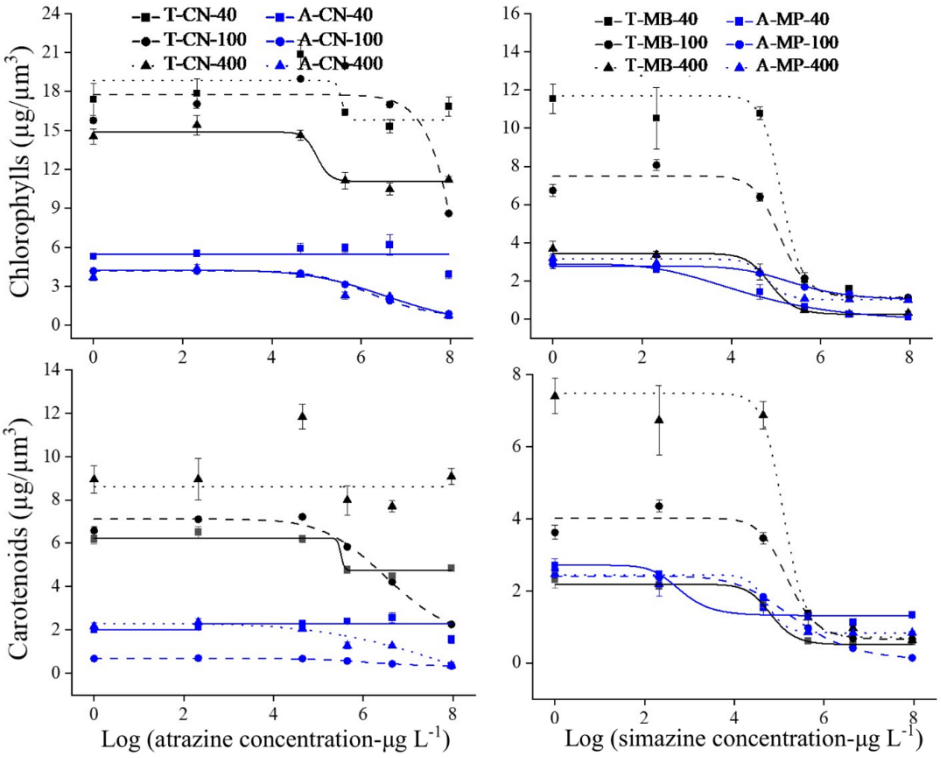


Figure 2. The effect of atrazine (after 72 h) on the pigment content of four microalgal species (temperate *C. neogracile* (T-CN), Arctic *C. neogracilis* (A-CN), temperate *M. bravo* (T-MB), and Arctic *M. polaris* (A-MP)) under LL (square), ML (circle) and HL (triangle) light intensities. The presented data calculated is relative to cell biovolume ($\mu m^3$), data expressed as means ± SD (n = 6).

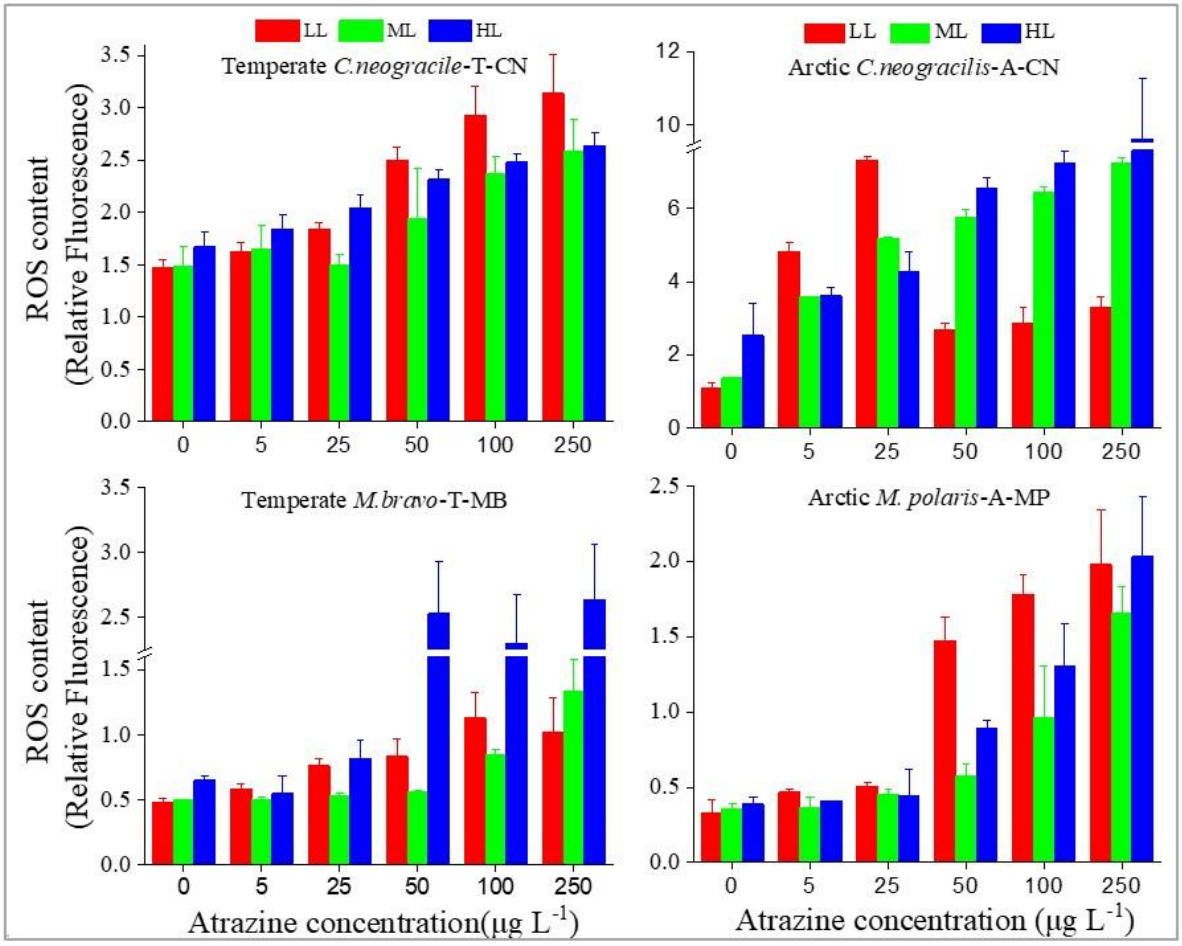


Figure 3. The effect of atrazine on ROS content of the studied species (temperate *C. neogracile* (T-CN), Arctic *C. neogracilis* (A-CN), temperate *M. bravo* (T-MB), and Arctic *M. polaris* (A-MP)) after 72 h exposure under LL, ML and HL. Data expressed as means ± SD (n = 6).

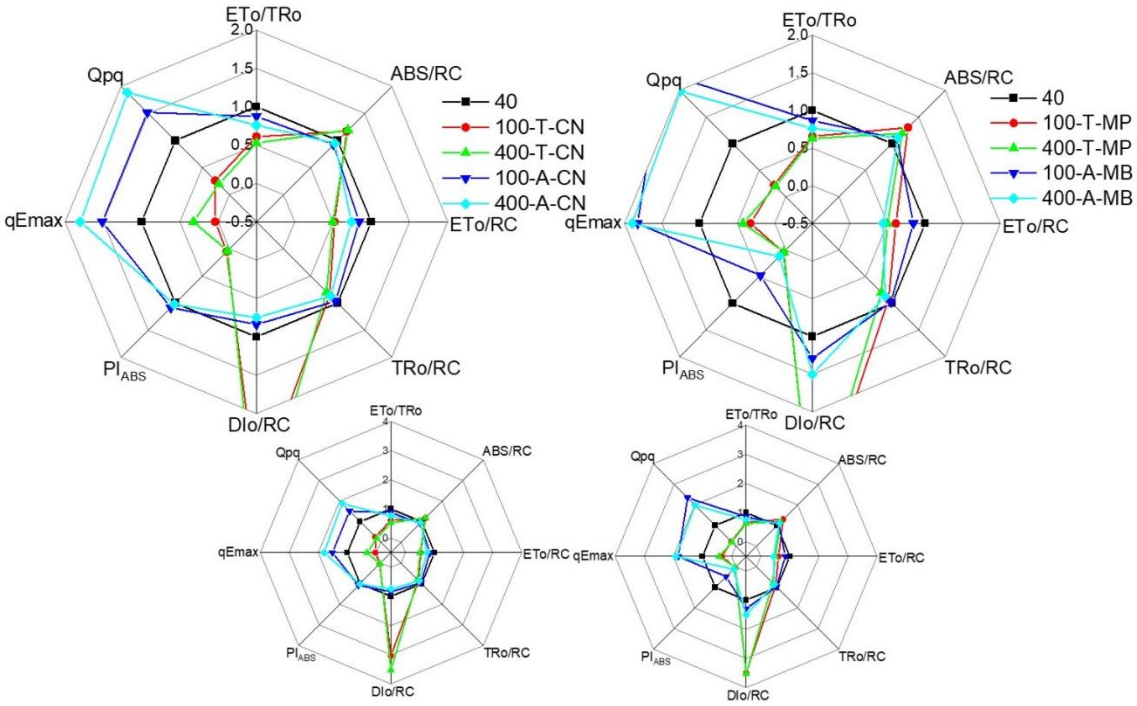


Figure 4. The effect of growth light intensity (LL, ML, and HL) on the PSII energy fluxes of temperate *C. neogracile* (T-CN), Arctic *C. neogracilis* (A-CN), temperate *M. bravo* (T-MB), and Arctic *M. polaris* (A-MP). Data expressed as means ± SD (n = 6).

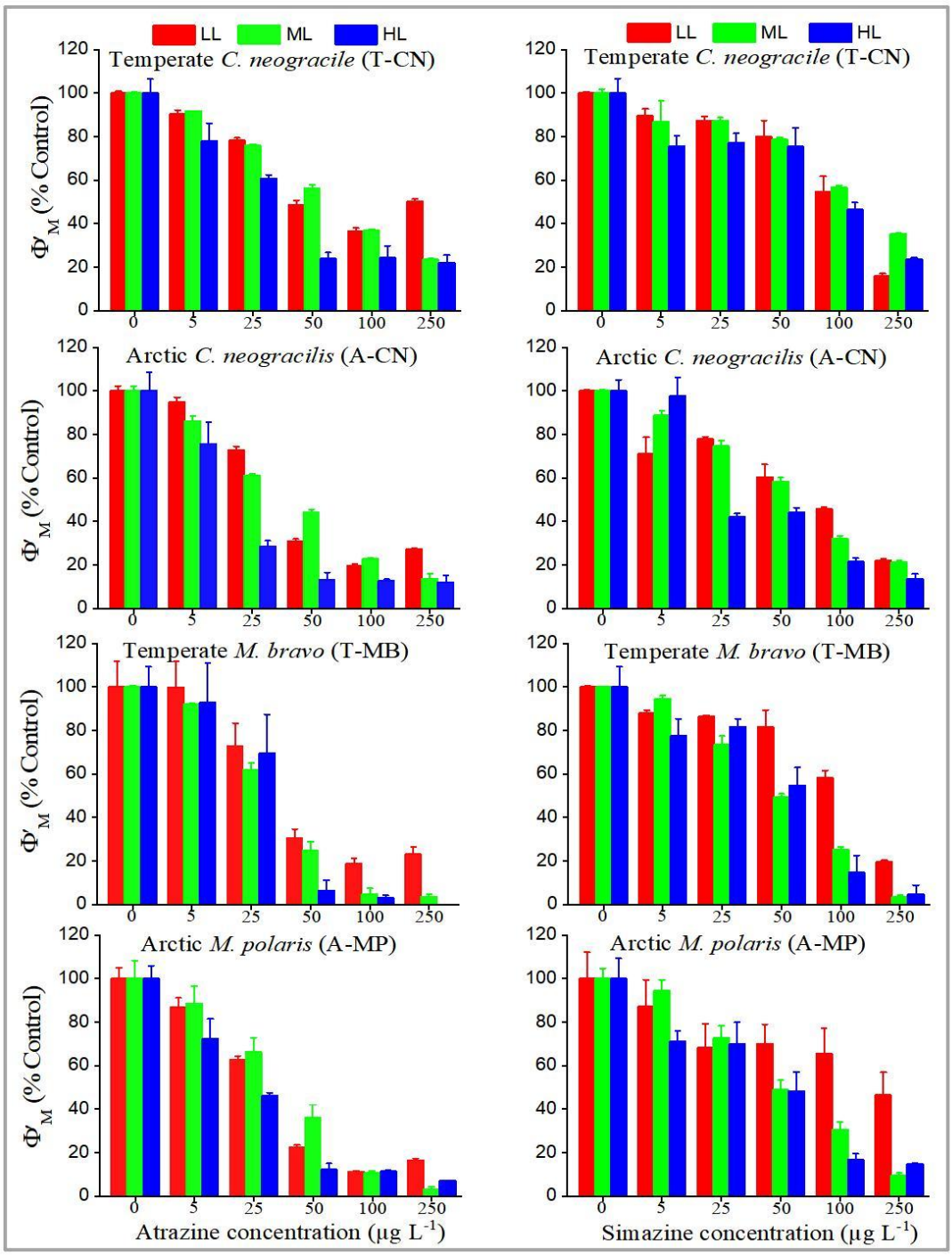


825

826 Figure 5. The effect of atrazine and simazine on the PSII operational quantum yield ($\Phi'_M$) of temperate *C.*
827 *neogracile* (T-CN), Arctic *C. neogracilis* (A-CN), temperate *M. bravo* (T-MB), and Arctic *M. polaris* (A-MP)
828 after 72 h exposure under LL, ML and HL conditions. Data expressed as means ± SD (n = 6).

829

830

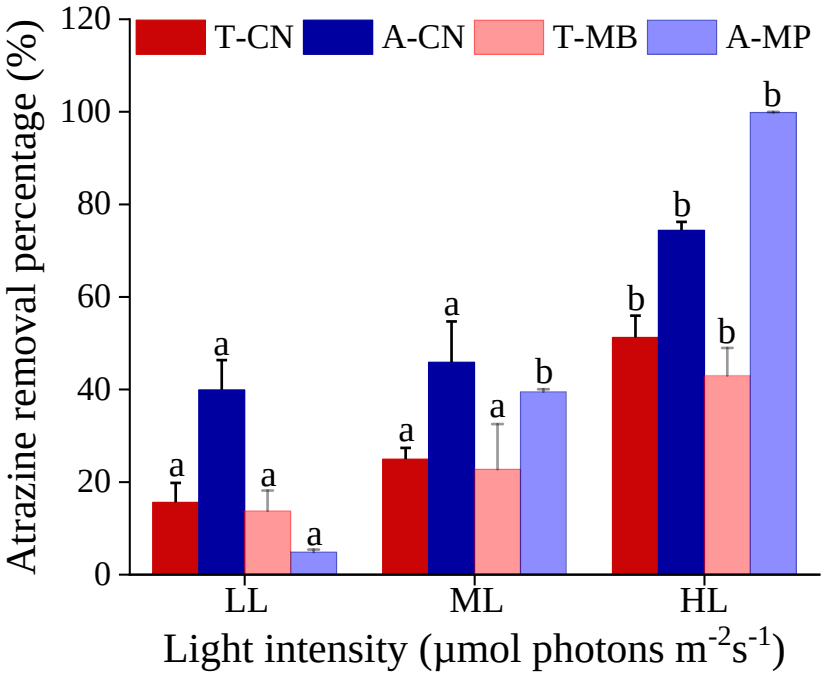


831

832 Figure 6. The concentration of atrazine removed from the growth medium for (red color) temperate *C.*
833 *neogracile* (T-CN) and temperate *M. bravo* (T-MB), (blue color) Arctic *C. neogracilis* (A-CN) and Arctic *M.*
834 *polaris* (A-MP) after 72 h exposure to 50 μg $L^{-1}$ under LL, ML and HL conditions. Data expressed as means
835 ± SD (n = 6).

836

# Supplementary Material

Figure S1. The effect of atrazine and simazine on the cell biovolume of the temperate *C. neogracile* (T-CN), Arctic *C. neogracilis* (A-CN), temperate *M. bravo* (T-MB), and Arctic *M. polaris* (A-MP) after 72 h exposure under LL, ML, and HL. Data expressed as means ± SD (n = 6).

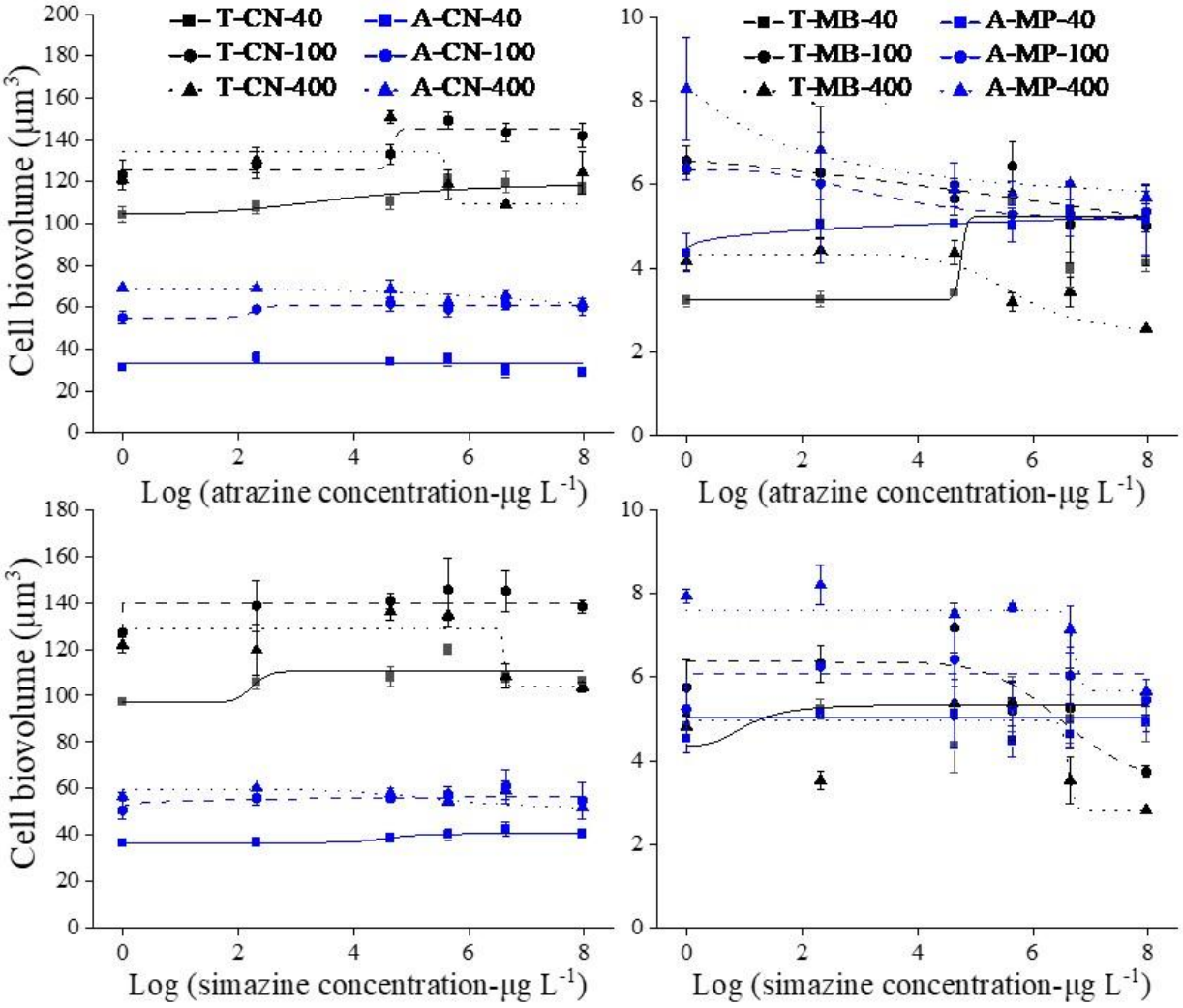

843 Table S1. In this study, parameters of fluorescence were defined.

| **Parameters** | **Definition** |
|---|---|
| $\Phi_M$ | Maximal PSII quantum yield |
| $\Phi'_M$ | Operational PSII quantum yield |
| NPQ | Non-photochemical quenching |
| NPQmax | Maximum ability for dissipation of excess energy |
| rETRmax | Maximum relative photosynthetic electron transport rate |
| α | Maximum light efficiency use |
| $E_K$ | Light saturation coefficient |
| **Specific energy fluxes (per $Q_A$ reducing PSII RC)** | |
| ABS/RC | Absorption flux (of antenna Chls) per RC (also a measure of PSII apparent antenna size) |
| TRo/RC | Trapped energy flux (leading to $Q_A$ reduction) per RC |
| ETo/RC | Electron transport flux (further than $Q_A^-$) per RC |
| DIo/RC | Dissipated energy flux per RC |
| **Performance index** | |
| $PI_{ABS}$=(RC/ABS) | Performance index (potential) for energy conservation from photons absorbed by PSII to the reduction of intersystem electron acceptors |

844